Environmental Fluid Mechanics (2005) 5: 495–505
DOI 10.1007/s10652-005-1052-8 © Springer 2006

Drift of an Inextensible Sheet Caused by Surface Waves

K.H. CHRISTENSEN* and J.E. WEBER
Department of Geosciences, University of Oslo, Oslo, Norway

Received 10 September 2004; accepted in revised form 20 January 2005

Abstract. Inextensible films are often used to simulate surface-active material as commonly found at sea. It is important to understand the mechanism behind wave-induced transport of surfactants with regard to e.g. oil spills in coastal areas. In this paper we compare theory, based on a Lagrangian description of motion, with observations of the wave-induced drift of thin inextensible plastic sheets in a controlled laboratory experiment. It is found that the analytical solution is able to reproduce the observed drift. In a laboratory situation with continuously generated, spatially damped waves, the drift velocity increases in time. Hence earlier theoretical treatments in which a steady state is assumed predict too low values of the drift velocity. The need for data on the time development of the drift is pointed out.

Key words: laboratory experiments, oil spill, surface film, surface waves, wave drift

1. Introduction

Objects floating on the sea surface in general possess a mean drift velocity caused by the joint action of wind, currents and waves. The role of waves is perhaps the least investigated, and if the object in question is a slick of surfactant, the problem becomes even more complicated because the wave-field is modified by the slick in the whole area it covers. The slick acts to restrict motion tangential to the surface and strong shear is produced in the viscous surface boundary layer, which ultimately leads to more rapid damping of the waves [1–3]. The momentum lost as oscillatory motion is regained as an Eulerian mean current by the diffusion of vorticity from the boundary layer [4]. This Eulerian mean current comes in addition to the inviscid Stokes drift [5], and the slick, being advected by the mean currents, may therefore have a drift velocity significantly higher than that predicted by Stokes theory.

A Lagrangian description of motion is particularly well suited for studying the wave-induced drift. It allows for a simple description of the free surface, and directly yields the particle drift. Although theoretical results

*Corresponding author, E-mail: k.h.christensen@geo.uio.no

for the wave-induced drift of inextensible and elastic surface films exist [6, 7], a validation of these results is difficult due to a lack of experimental data. Field studies cannot be used for validation purposes, as both the effects of wind and an irregular wavefield are not accounted for in the analyses. Furthermore, one of the basic assumptions in the above-mentioned theoretical studies is that the film cover is continuous, whereas the few conducted laboratory studies has focused on the drift of films of limited size (with width and length just a fraction of the wavelength, say), which cannot modify the waves to any extent [8, 9]. In other laboratory studies the absence of important information, for example the duration time of the experiment, makes a comparison between experiment and theory impossible [10–12]. In a typical laboratory experiment, waves are generated in one end of a wave tank, and the surface film is let free to drift. The waves will attenuate in space rather than time, and since momentum is continuously put into the system, the source of Eulerian mean momentum is unlimited. Accordingly, the Eulerian mean current will increase in time [13].

A notable exception among the existing laboratory studies is the study by Law [14] of the wave-induced drift of thin rectangular polypropylene sheets. Three requirements for comparing Law's data with existing theory are fulfilled: (i) the sheets were large enough to modify the waves, justifying the use of the mathematical model, (ii) all the necessary wave parameters were reported, (iii) the approximate duration time of the experiments can be deduced. Law also presented a theoretical analysis, based on Phillips [15]. However, assuming that the vorticity is confined to the surface boundary layer, Law's analysis does not capture the time development of the drift current. The observed drift velocities are in general found to be higher than predicted by Law's theory.

In this paper, we compare the experimental results of Law with the theoretical results of Weber [16]. The outline of the paper is as follows: In Section 2 we present an analytical solution for inextensible films of finite length. In Section 3 we compare the solution with drift data from Law, while Section 4 contains some concluding remarks and recommendations for future laboratory studies.

2. Analytical Solution in Lagrangian Description

We simplify and take the problem to be two-dimensional. The waves are monochromatic and continuously generated. An inextensible, freely drifting film of length L covers a part of the water surface, which is otherwise free from any surfactants. The waves enter the film with an amplitude ζ_0 and are damped as they propagate through the film. The surface is assumed to be free from any external stresses, thus we neglect the presence of air above the film. The validity of this assumption will be discussed later on.

We use a Lagrangian description of motion. The spatial coordinates (a, c) denote the fluid particles initial horizontal and vertical position, respectively, in a Cartesian coordinate system. The vertical axis is positive upwards and the free surface is given by $c=0$ at any time, t. The dependent variables are expanded in perturbation series and inserted in the equations of motion and continuity [17]. The parameter of expansion is taken proportional to the wave slope $\zeta_0 k$, where k is the wave number. We will need to pursue our calculations to $O((\zeta_0 k)^2)$ to obtain the wave-induced drift.

A detailed derivation of the equations for the drift velocities in spatially damped waves can be found in Weber [16]. Although Weber considered water covered by grease ice, the formulation is applicable for water covered by an inextensible film (see [6] for the case of temporally damped waves and inextensible film, and e.g. [18] for both spatially and temporally damped waves in a film-free rotating ocean). For deep-water gravity waves with wave frequency ω, the equation for the mean horizontal drift velocity u, in a non-rotating system, is

$$u_t - \nu u_{cc} = -u_S \nu k^2 \left\{ 4e^{2kc} + 3\frac{\gamma^2}{k^2} e^{2\gamma c} + 4\frac{\gamma^2}{k^2} e^{\gamma c} \sin \gamma c \right\} e^{-2\alpha a}. \quad (1)$$

Here ν is the kinematic viscosity, $u_S = \zeta_0^2 \omega k$ is the surface value of the inviscid Stokes drift, $\gamma = \sqrt{\omega/(2\nu)}$ is the inverse boundary layer thickness, and $\alpha = k^2/(2\gamma)$ is the spatial attenuation coefficient for inextensible films. Furthermore, we have let subscripts denote partial differentiation. The derivation of (1) is based on the assumption that the boundary layer width is much smaller than the wavelength, that is $k/\gamma \ll 1$, a requirement that is very well fulfilled for gravity waves. For wave lengths of 1.5 meters the corresponding boundary layer width is approximately 0.6 mm, which means that $k/\gamma = O(10^{-3})$.

It proves convenient to separate u into three parts,

$$u = u^{(S)} + u^{(\nu)} + u^{(E)}. \quad (2)$$

The first two parts on the righthand side of (2) is given by the particular solution of (1), with $u^{(S)}$ representing the inviscid Stokes drift and $u^{(\nu)}$ a vorticity solution confined to the surface boundary layer. The homogeneous solution of (1) represents the transient Eulerian mean current, $u^{(E)}$, resulting from diffusion of vorticity from the surface. We find from (1):

$$u^{(S)} = u_S e^{2kc - 2\alpha a}, \quad (3)$$

$$u^{(\nu)} = u_S \left(\frac{3}{4} e^{2\gamma c} - 2e^{\gamma c} \cos \gamma c \right) e^{-2\alpha a}. \quad (4)$$

With negligible mass, the film cannot support any net stress acting on it. In the absence of any external stresses, the appropriate boundary condition at the surface is therefore that the mean Lagrangian shear stress is zero [4, 7]:

$$\rho \nu u_c = 0, \quad c = 0. \tag{5}$$

Here ρ is the fluid density.

For continuously generated waves and infinite water depth the source of second-order mean momentum is unlimited. The waves constantly produce vorticity in the boundary layer, and the resulting mean stress this vorticity exerts on the surface must be balanced in order for (5) to be fulfilled. The balancing stress is due to the Eulerian mean current and is formally known as the virtual wave stress, τ_w [19]. In our Lagrangian framework the virtual wave stress is defined as

$$\tau_w = \rho \nu u_c^{(E)}(c=0) = -\rho \nu u_c^{(\nu)}(c=0), \tag{6}$$

where the last equality follows from (2) and (5). Strictly speaking, the contribution from the Stokes drift should be included in (6), but this contribution is of $O(k/\gamma)$ compared to the contribution from $u^{(\nu)}$ and therefore neglected. From (4) and (6) we obtain

$$\tau_w = \frac{1}{2} \rho \nu \gamma u_S e^{-2\alpha a}. \tag{7}$$

Now consider a situation where the sheet is not allowed to drift freely, but is kept stagnant by a resisting force. The force $\mathcal{F}$ required to keep a sheet of surface area $\mathcal{A}$ from drifting can be written [16]

$$\mathcal{F} = -\int_{\mathcal{A}} \tau_w \, d\mathcal{A}. \tag{8}$$

Experiments by Kang and Lee [11] show that there is excellent agreement between Equation (8) and the measured wave-induced drag on an inextensible sheet kept stagnant.

We may now formulate the problem for $u^{(E)}$. From (1)–(6), assuming that the depth is such that the drift velocity never reaches the bottom, we find that the time development of the mean Eulerian drift current is determined by [13]

$$u_t^{(E)} = \nu u_{cc}^{(E)}, \tag{9}$$

$$u_c^{(E)} = \frac{\tau_w}{\rho \nu}, \quad c = 0, \tag{10}$$

$$u^{(E)} \to 0, \quad c \to -\infty. \tag{11}$$

It follows from (7) and (10) that τ_w provides a time independent source of Eulerian mean momentum.

The derivation of (1) is based on the assumption that the wavefield is immediately established. The Stokes drift is an inherent part of irrotational wave motion, hence a straightforward choice of initial condition for u is

$$u = u^{(S)}, \quad t = 0. \tag{12}$$

Using (2) and (12), the corresponding initial condition for $u^{(E)}$ becomes

$$u^{(E)} = -u^{(\nu)}, \quad t = 0. \tag{13}$$

The Equations (9)–(11) and (13) now completely determine the Eulerian mean current.

We denote average values for a film of length L by using capital letters, i.e.

$$U \equiv \frac{1}{L}\int_0^L u\, da. \tag{14}$$

The solution to (9)–(11), applying (13), can be found by the method of Laplace transforms. For a film of finite length we obtain

$$\begin{aligned} U^{(E)} = Au_S\Bigg\{ &\frac{1}{2}\left(\frac{\omega}{2\pi}\right)^{1/2}\int_0^t \frac{\exp\{-c^2/(4\nu\xi)\}}{\sqrt{\xi}}d\xi \\ &+\frac{(2\omega)^{1/2}}{\pi}\int_0^\infty \left[\frac{\xi+\omega}{\xi^{1/2}(\xi^2+\omega^2)} - \frac{3}{4\xi^{1/2}(\xi+2\omega)}\right] \\ &\times\, e^{-\xi t}\cos(c\xi^{1/2}/\nu^{1/2})d\xi\Bigg\}, \end{aligned} \tag{15}$$

where $A = (1-\exp\{-2\alpha L\})/(2\alpha L)$. The coefficient A expresses the dependence on the relative amplitude damping over the film. For short films or weak damping we have A close to unity, and for very long films or heavily damped waves the value of A approaches zero. The solution (15) describes an accelerating Couette type flow, driven by the virtual wave stress acting on the surface. At each depth the velocity increases in time by the downward diffusion of momentum. The Stokes drift and boundary layer solution are then added to (15) to obtain the total velocity profile. The drift velocity of the film equals the surface value of U, from (3), (4) and (15) we obtain

$$U_0 = U(c=0) = Au_S\left\{\sqrt{t/T} - 1/4 + \frac{(2\omega)^{1/2}}{\pi}\int_0^\infty \left[\frac{\xi+\omega}{\xi^{1/2}(\xi^2+\omega^2)} - \frac{3}{4\xi^{1/2}(\xi+2\omega)}\right]e^{-\xi t}d\xi\right\}, \quad (16)$$

where $T = 2\pi/\omega$ is the wave period.

The derivation of (16) is based on the assumption that the film is so long that it can actually modify the waves. Short films with $L \ll \lambda$, where λ is the wavelength, will not be able to damp the waves to any extent, in which case Equation (1) will not hold. Such films will rather be advected by the drift current as induced by waves on clean surfaces. Even with a clean surface the drift velocity can exceed the classic inviscid Stokes drift due to the damping effect of air [13]. In our case the effect of the film will dominate. An inextensible film is very effective in suppressing surface waves, for waves with a period of one second the loss in amplitude is 40% in 100 m. Without any film (but including the damping effect of air), the amplitude reduction is 1.3%. The virtual wave stress τ_w from (7) is of $O(\gamma/k)$ larger than the virtual wave stress in the case of air over a clean surface, justifying our assumption that the effect of air can be neglected.

3. Comparison with Laboratory Experiments

3.1. DESCRIPTION OF THE EXPERIMENTS

Law [14] used a wave tank 45 m long, 1.6 m wide and with a water depth of 3 m. Rectangular pieces of 0.08 mm thick polypropylene, 1.2 m wide and of varying length, were placed transversally centered on the surface initially at rest. Upon generating waves with a period $T = 1$ s, the subsequent drift of the sheets was recorded by a video camera. The corresponding wavelength would be that of deep water waves, with $\lambda = 1.56$ m, and a phase velocity $\lambda/T = 1.56$ m/s.

Experiment duration time. Data collection were restricted to the time interval determined by two criteria: (i) after at least five waves had passed, and, (ii) before the reflected waves arrived back at the measurement area. The experiments in general lasted 20–60 s from the onset of the wave maker, but these figures are approximate since there were variations between each experimental run (Law, private communication, 2004). Because it would take a few wave cycles before the wave maker produced uniform waves, and since the waves would take some time to reach the measurement area, the corresponding time the sheets were subjected to the waves should be approximately 10–50 s. Given the wave period of one second, the first criterion for data collection imply that the shortest possible time for which a sheet were allowed to drift would be $t = 5$ s. A longest possible drift time $t = 50$ s is consistent with the time required for a wave to propagate from the measurement area, reflect at the far end of the wave tank, and propagate back to the measurement area.

Length of sheet. The ratio between sheet length and wavelength were varied from $L/\lambda = 0.2$–3 in Law's experiments, though only results for the sheets with $L/\lambda \geq 0.8$ are presented. The value of the coefficient A is between 1 and 0.98 for L/λ between 0 and 3, with $\lambda = 1.56$ m. Hence for the sheets used by Law we can safely set $A = 1$. The drift velocity should therefore be practically the same for any two films with L/λ between some value $(L/\lambda)_{\min}$ and 3, as long as the dynamics can be considered as well described by Equation (1). The pertinent question is then for which minimum value of $(L/\lambda)_{\min}$ we can expect the solution (16) to become valid? Law states that the dependence of sheet length becomes less significant for $L/\lambda > 0.8$. Kang and Lee [12] conducted a series of experiments, much similar to those of Law, but do not give sufficient details on the experiments for us to use them in this study. However, they report that the drift velocity seems to become more or less independent on the sheet length for $L/\lambda > 1.5$. For the comparison we will use the data for the longer sheets with $L/\lambda = 2, 2.5$ and 3.

3.2. RESULTS

Considering the experimental setup, computing the drift velocity from the observed displacement of the sheet requires some form of time averaging, where the distance covered by the sheet is measured in a certain time interval. This time interval may be chosen differently for each sheet. If the time interval is short, the computed drift velocity would resemble the instantaneous drift velocity. According to our solution (16), the sheets accelerate at all times and no steady state occurs. In consequence, if the displacement of the sheet is measured at the beginning of the experiment, a lower value for the drift velocity is expected compared to the case where the displacement is measured towards the end of the experiment. If the time interval is long, the computed drift velocity should in any case lie between the lower and upper bounds defined by the instantaneous drift velocity at the times given by the shortest and longest experiment duration time, respectively. Another aspect related to the required time averaging is discussed in Section 3.3.

The observed drift velocities from Law's experiments are shown in Figure 1, with the solution from (16) for $t = 5$, 10 and 50 s, using $A = 1$. Note that the drift velocities are in general several times higher

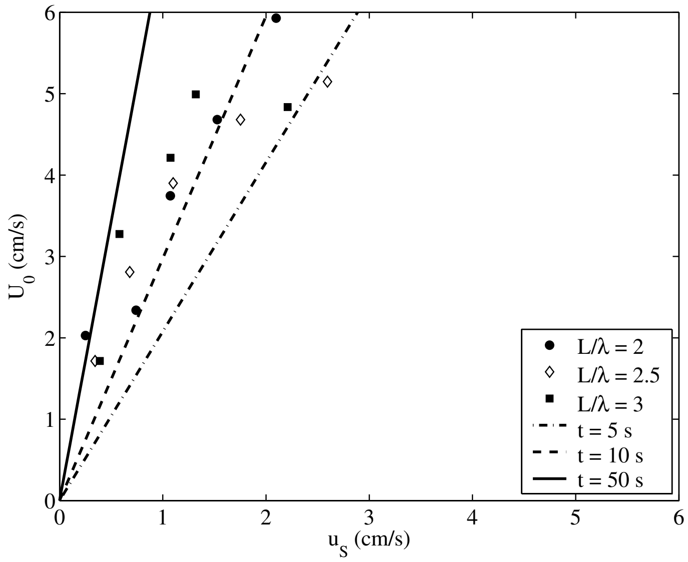

Figure 1. Observed drift velocities of inextensible plastic sheets from Law [14] and theoretical predictions from (16). $u_S = \zeta_0^2 \omega k$ is the surface value of the classic inviscid Stokes drift.

than predicted by Stokes theory. All but two data points are within the theoretical bounds defined by the solution (16) evaluated at $t = 5$ s and 50 s. There is considerable spread in the experimental data, which is to be expected because the duration times varied over a relatively large interval. What is most important is that the solution (16) predicts such high drift velocities as observed in the experiments. It is clear that one has to take into account the transient part of the drift current to obtain realistic values. The observed drift velocities are often 1.5–2 times higher than predicted by the steady state solutions of both Law and Phillips [15].

In another set of experiments, Wong and Law [9] investigated the drift of sheets of elliptical shape. Our theoretical results are not applicable since these sheets were relatively small compared to the waves. However, Wong and Law observed that the longer sheets ($L/\lambda > 0.65$) accelerated, and in some experimental runs, the drift velocity was found to be increasing even after the reflected waves theoretically interfered with the incident waves. The energy of the reflected waves was small due to an absorbent beach at the far end of the wave tank, but the point is that the sheets did accelerate during the whole experimental run, and did not attain a steady drift velocity. According to our solution (16), the acceleration will decrease after some time. The relative increase in drift speed between 40 and 50 wave periods after the onset of motion is approximately ten percent. In a laboratory situation, such a small velocity increase after an initial large acceleration may appear as a steady state, keeping in mind that the mean drift velocity comes in addition to the orbital velocity of the waves.

3.3. APPARENT LINEARITY IN EXPERIMENTAL DATA

Our solution (16) predicts that U will increase quadratically with the wave steepness. However, in some experimental studies, including the study by Law, the observed drift velocities of long sheets show an almost linear growth with $\zeta_0 k$ (e.g. Kang and Lee [12]). These observations do not necessarily contradict our result (16), but may be explained as artifacts of the experimental procedure. Alofs and Reisbig [8] describe how they computed the drift velocity based on the observed displacement of the film, a method which one may assume is used by others: The film is placed a fixed distance D_1 from the measurement area, initially at rest, and the wave maker is started. The film drifts into the measurement area, of fixed length D_2, after a time t_1, and leaves the measurement area after a time t_2 (both t_1 and t_2 are measured from the onset of the waves). An average drift velocity can then be computed as

$$U_{\text{av}} = D_2/(t_2 - t_1). \tag{17}$$

Given values of D_1 and D_2 one can compute t_1 and t_2, and hence U_{av}, from the theoretical solution (16), and check whether the result is quadratic in $\zeta_0 k$ or not. The full expression in (16) is somewhat difficult to manipulate, but after a short while ($t \sim T$) we have approximately

$$U = A u_S \sqrt{t/T}. \tag{18}$$

Using (18) as the theoretical drift velocity, and letting $A = 1$ as before, we obtain

$$U_{\text{av}} = (\zeta_0 k)^{4/3} B_1 B_2, \tag{19}$$

where

$$B_1 = \left(\frac{2\omega^3}{9\pi k^2}\right)^{1/3}, \quad B_2 = \frac{D_2}{(D_1 + D_2)^{2/3} - D_1^{2/3}}. \tag{20}$$

We note from (19) that U_{av} becomes proportional to $(\zeta_0 k)^{4/3}$, hence if one uses the measuring technique of Alofs and Reisbig, one should expect to find an almost linear growth of U with increasing wave steepness. While B_1 depends on the wave characteristics, B_2 will vary depending on the setup of the experiment. It should be noted that B_1 varies slowly with the wave frequency, for gravity waves we have $B_1 \sim \omega^{-1/3}$. Thus if a narrow range of wave frequencies is used in a particular set of experiments, the product $B_1 B_2$ will be approximately constant.

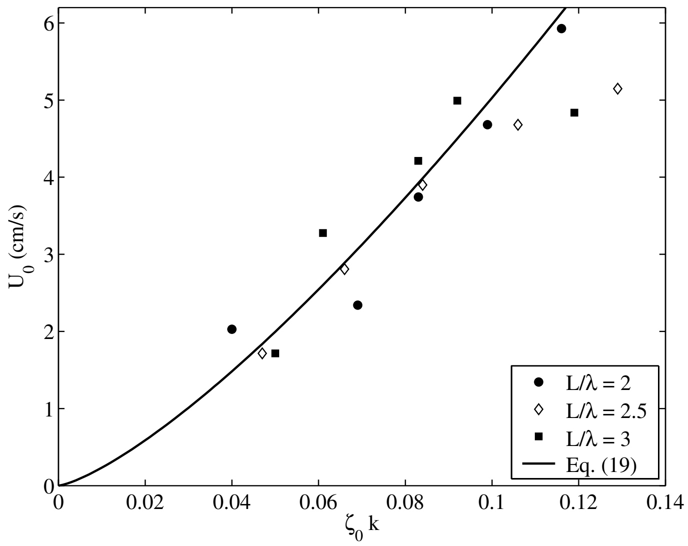

Figure 2. Observed drift velocities of inextensible plastic sheets from Law [14] and the theoretical prediction from (19). Here we have used $D_1 = 30$ cm and $D_2 = 10$ cm.

The measuring technique used by Law differs from that of Alofs and Reisbig in the sense that the values of D_1 and D_2 both would vary between the experimental runs (Law, private communication, 2004). It is tempting, however, to compare (19) to Law's data, choosing reasonable values for D_1 and D_2. A comparison with other, similar studies has not been possible due to lack of detail on the experimental setup. Figure 2 shows the observed drift velocities from Law's experiments and the theoretical solution from (19) using $D_1 = 30$ cm and $D_2 = 10$ cm. These values for the drift distances are consistent with the duration of the experiments and the observed drift velocities. It seems that Equation (19) describes well the trend for increasing wave steepness.

4. Concluding Remarks

In this paper we have compared the theoretical analysis of Weber [16] with the observed wave-induced drift of inextensible sheets as reported by Law [14]. The time-dependent solution we present predicts the high drift velocities observed in the experiments. This is in contrast to the steady-state solutions of Law and Phillips [15], which underestimate the drift. Because most experimental data, like those reported by Law, are given as time averages, it has not been possible to compare the predicted time development of the drift with observations. Data on the temporal variation of the wave-induced surface drift is desirable, and we strongly recommend that this is taken into account in future laboratory studies.

Acknowledgments

The authors wish to thank Dr Adrian W.K. Law for providing more detailed information on his experiments. K.H. Christensen gratefully acknowledges financial support from The Research Council of Norway through Grant No. 151774/432.

References

1. Lamb, H.: 1932, *Hydrodynamics*. Cambridge University Press.
2. Dorrestein, R.: 1951, General linearized theory of the effect of surface films on water ripples, *Proc. K. Ned. Akad. Wet., Ser. B: Phys. Sci.* **B54**, 260–272,350–356.
3. Jenkins, A.D. and Jacobs, S.J.: 1997, Wave damping by a thin layer of viscous fluid, *Phys. Fluids* **9**(5), 1256–1264.
4. Longuet-Higgins, M.S.: 1953, Mass transport in water waves, *Philos. Trans. R. Soc. London, Ser. A* **245**, 535–581.
5. Stokes, G.G.: 1847, On the theory of oscillatory waves, *Trans. Camb. Phil. Soc.* **8**, 441.
6. Weber, J.E. and Førland, E.: 1989, Effect of an insoluble surface film on the drift velocity of capillary-gravity waves, *J. Phys. Oceanogr.* **19**(7), 952–961.
7. Weber, J.E. and Saetra, Ø.: 1995, Effect of film elasticity on the drift velocity of capillary-gravity waves, *Phys. Fluids* **7**(2), 307–314.
8. Alofs, D.J. and Reisbig, R.L.: 1972, An experimental evaluation of oil slick movement caused by waves, *J. Phys. Oceanogr.* **2**, 439–443.
9. Wong, P.C.Y. and Law, A.W.K.: 2003, Wave-induced drift of an elliptical surface film, *Ocean Engng.* **30**, 413–436.
10. Lange, P. and Hühnerfuss, H.: 1978, Drift response of monomolecular slicks to wave and wind action *J. Phys. Oceanogr.* **8**, 142–150.
11. Kang, H.K. and Lee, C.M.: 1995, Steady streaming of viscous surface layer in waves, *J. Mar. Sci. Technol.* **1**, 3–12.
12. Kang, H.K. and Lee, C.M.: 1996, Prediction of drift in a free surface, *Ocean Engng.* **23**(3), 243–255.
13. Weber, J.E.: 2001, Virtual wave stress and mean drift in spatially damped surface waves, *J. Geophys. Res.* **106**(C6), 11653–11657.
14. Law, A.W.K.: 1999, Wave-induced surface drift of an inextensible thin film, *Ocean Engng.* **26**, 1145–1168.
15. Phillips, O.M.: 1977, *The Dynamics of the Upper Ocean*. Cambridge University Press.
16. Weber, J.E.: 1987, Wave attenuation and wave drift in the marginal ice zone, *J. Phys. Oceanogr.* **17**(12), 2351–2361.
17. Pierson, W.J.: 1962, Perturbation analysis of the Navier-Stokes equations in Lagrangian form with selected linear solutions, *J. Geophys. Res.* **67**(8), 3151–3160.
18. Jenkins, A.D.: 1986, A theory for steady and variable wind- and wave-induced currents, *J. Phys. Oceanogr.* **16**(8), 1370–1377.
19. Longuet-Higgins, M.S.: 1969, A nonlinear mechanism for the generation of sea waves, *Proc. Roy. Soc. A.* **311**, 371–389.